

## Combined effects of pressure, temperature, and magnetic field on the ground state of donor impurities in a GaAs/AlGaAs quantum heterostructure

Samah Abuzaid, Ayham Shaer, Mohammad Elsaid\*

Department of Physics, An-Najah National University, Nablus, West Bank, Jordan

Received 09 February 2019; revised 15 July 2019; accepted 20 July 2019; available online 30 July 2019

### Abstract

In the present work, the exact diagonalization method had been implemented to calculate the ground state energy of shallow donor impurity located at finite distance along the growth axis in GaAs/AlGaAs heterostructure in the presence of a magnetic field taken to be along z direction. The impurity binding energy of the ground state had been calculated as a function of confining frequency and magnetic field strength. We found that the ground state donor binding energy (BE) calculated at  $\omega_c = 2R^*$  and  $\omega_0 = 5.421R^*$ , decreases from  $BE = 7.59822 R^*$  to  $BE = 2.85165 R^*$ , as we change the impurity position from  $d = 0.0 a^*$  to  $d = 0.5 a^*$ , respectively. In addition, the combined effects of pressure and temperature on the binding energy, as a function of magnetic field strength and impurity position, had been shown using the effective-mass approximation. The numerical results show that the donor impurity binding energy enhances with increasing the pressure while it decreases as the temperature decreases.

**Keywords:** Binding Energy; Donor Impurity; Exact Diagonalization Method; Heterostructure; Magnetic Field.

### How to cite this article

Abuzaid S, Shaer A, Elsaid M. Combined effects of pressure, temperature, and magnetic field on the ground state of donor impurities in a GaAs/AlGaAs quantum heterostructure. *Int. J. Nano Dimens.*, 2019; 10 (4): 375-390.

### INTRODUCTION

Low dimensional heterostructure have been studied intensively in the last decades, both theoretically and experimentally [1-3]. Quantum confined semiconductor systems such as quantum well (QW), quantum well wire (QWW), quantum dots (QD) and quantum rings (QR) are important elements in the present electronic devices. The electrical, optical and transport properties of these semiconductor heterostructure systems can be changed by external effects like: donor impurities near the heterostructure surface, electric field, magnetic field, pressure, and temperature [3,4]. Moreover, the effect of the donor impurity on the properties of the heterostructure materials is very interesting subject which has been investigated. Adding the donor impurity atoms change the effective charge and mass of it, which alter the performance of the quantum devices and the transport properties [5]. The binding energy

of the impurity and the coulombic interaction between the system charge carrier and the donor impurity change the heterostructure energy gap [6, 7]. The donor impurity binding energy had been investigated from bulk to the quantum dot where it depends on the dimensionality of the system, shape, and the impurity position [1, 8, 9]. Also, it is affected the heterostructure properties by the presence of the magnetic or electrical fields, pressure, and temperature [9, 10]. For the quantum dot, the donor impurity binding energy increases continuously with decreasing the dot radius, and the applied magnetic field strength, in addition, it depends on the impurity position [11, 12].

The donor binding energy had been studied for the quantum well by using variation method, where the ground state of donor binding energy had been computed as a function of the impurity position and the QW width under different electric

\* Corresponding Author Email: [mkelsaid@najah.edu](mailto:mkelsaid@najah.edu)

field strengths [13, 14]. The donor impurity energy for the ground and excited state of two-dimensional heterostructure had been computed as a function of magnetic field strength, for both weak and strong magnetic field limit, using exact and perturbation methods [15]. Chuu *et al.* in Ref. [16] obtained the donor impurity energy levels analytically for both donor impurity located at the quantum dots center, and for donor impurity located at the axis of the quantum-well wire. Zhu and Gu in Ref. [17] investigated the dependence of the energy transition on shallow donor impurity states in a harmonic QD by using analytical method with the presence of the magnetic field. The energy transition changes with the magnetic field strength, where the result shows the high effects of magnetic fields on donor impurity energy states transition [17]. The dependence of the diamagnetic susceptibility and the binding energy of the donor impurity on the pressure and the temperature had been shown analytically. Khordad and Fathizadeh found in their recent study the diamagnetic susceptibility increases by increasing the pressure and it decreases with increasing the temperature [18]. Peter in Ref. [19] reported the binding energy levels of shallow hydrogenic impurities in a parabolic quantum dot (QD) with pressure effect using variation approach. Where, they are found that the ionization energy, is purely pressure-dependent. Merchancano *et al.* in Ref. [2] had also calculated the binding energy of the hydrogenic impurities in a spherical QD using the variation and perturbation approaches as a function of pressure, QD size, and the impurity position. The results of the study show that the binding energy increases with increasing the pressure [20]. The combined effects of pressure and temperature on the binding energy of donor impurity in a spherical QD with the presence of the electric field or without had been investigated [5, 21].

The exact diagonalization method had been used to solve the problem of two interacting electrons in the QD including the pressure and temperature effects. The magnetization and magnetic susceptibility of confined electrons in parabolic quantum dot was considered in both: experimental and theoretical studies [22, 23]. Very recently, Elsaid *et al.* [24-32], has studied the electronic, thermodynamic and magnetic properties of two electrons confined in a single quantum and coupled quantum dots

(CQD). Alfonso *et al.* in [33] had investigated the energy states of an electron confined in a two-dimensional (2D) plane and bound to an off-plane shallow donor center in the presences of an external magnetic field by using variation and numerical approaches. The effect of impurity on energy levels in double quantum rings had been considered by Khajeh Salehani *et al.* [34].

In this work, we have investigated the combined effects of pressure, temperature, magnetic field strength and the impurity position on the ground state binding energy of the donor impurity in heterostructure materials. We have computed the ground state energy level of donor impurity in a heterostructure by solving the donor impurity Hamiltonian using exact diagonalization method. The Hamiltonian theory of donor impurity located along the growth axis under the effect of a magnetic field, pressure and temperature had been presented, followed by numerical results and discussion. The conclusion is given at the end of the work.

## THEORY

This section describes the main parts of the donor impurity formulation: i) the quantum heterostructure Hamiltonian, ii) the exact diagonalization method and iii) the pressure and temperature effects on the computed donor impurity ground state binding energy by the effective-mass approximation. The system is a quantum heterostructure confined in the x-y plane with parabolic confinement potential of confining strength  $\omega_0$ ,  $V(r) = \frac{1}{2}m^*\omega_0^2r^2$ , and in the presence of a donor impurity along the z- axis located at distance d, under the influence of a uniform magnetic field strength,  $B = \nabla \times A$ , applied along the z -direction.  $A = \frac{B}{2}(-y, x, 0)$  is the vector potential.

The interaction between the electron in the GaAs layer and the donor impurity, located at distance d along the z-direction in AlGaAs barrier, is attractive coulomb interaction energy. The Hamiltonian of the donor impurity can be written in an operator form as:

$$\hat{H} = - \left( \rho^{-1/2} \frac{\partial^2}{\partial \rho^2} \rho^{1/2} + \frac{1}{\rho^2} \left( \frac{\partial^2}{\partial \phi^2} + \frac{1}{4} \right) \right) + \frac{1}{4} \omega^2 \rho^2 - i \frac{\omega_c}{2} \frac{\partial}{\partial \phi} - \frac{2}{|\mathbf{r} - \mathbf{d}|} \quad (1)$$

$\hat{H}$  in Eq. (1) can be separated into two parts as:

$$\hat{H} = \hat{H}_\perp + V(\rho) \tag{2}$$

where:

$$\hat{H}_\perp = - \left( \rho^{-1/2} \frac{\partial^2}{\partial \rho^2} \rho^{1/2} + \frac{1}{\rho^2} \left( \frac{\partial^2}{\partial \phi^2} + \frac{1}{4} \right) \right) + \frac{1}{4} \omega^2 \rho^2 - i \frac{\omega_c}{2} \frac{\partial}{\partial \phi} \tag{3}$$

and,

$$V(\rho) = - \frac{2}{|\rho - d|} = - \frac{2}{\sqrt{\rho^2 + d^2}} \tag{4}$$

The potential  $V(\rho)$  represents the coulomb interaction between the electron in the GaAs layer and the impurity ion, located at distance  $d$  along the z-direction in AlGaAs barrier screened

by the dielectric constant of GaAs medium. The Hamiltonian  $\hat{H}_\perp$  is a harmonic oscillator type with well-known solution. The effective confinement frequency, is a combination of the magnetic field cyclotron frequency and parabolic confining frequency, given as:  $\omega^2 = \omega_0^2 + \frac{\omega_c^2}{4}$ . Generally, there is no analytical solution available for the complete donor impurity Hamiltonian. In this work, we will use the exact diagonalization technique to solve the donor impurity Hamiltonian given by Eq. (1) and study its electronic properties.

For zero donor impurity case  $\hat{H}_\perp$ , Eq. (1) reduces to harmonic oscillator type with a well-known eigenstates  $|n,m\rangle$  and eigenenergies. The adopted basis ( $|n,m\rangle = \psi_{n,m}(\rho, \phi)$ ) are harmonic oscillator type wave functions that have been used to diagonalize the total Hamiltonian and obtain the ground state energy of the impurity system.

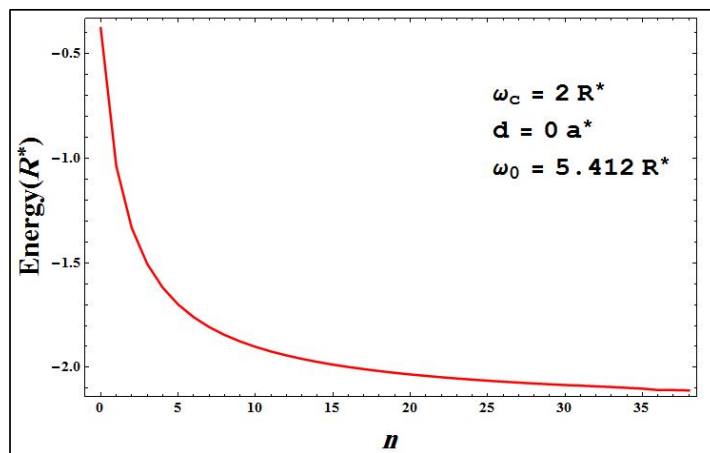


Fig. 1.a

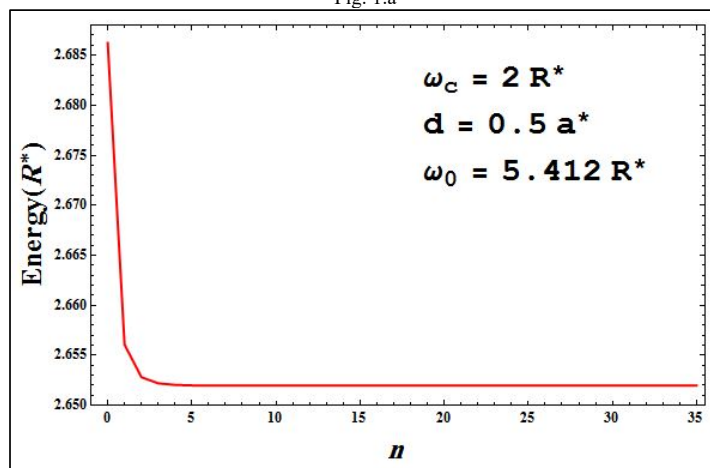


Fig. 1.b

Fig. 1. The ground state energy of the quantum heterostructure for fixed value of magnetic field strength ( $\omega_c = 2 R^*$ ) and parabolic confinement strength  $\omega_0 = 5.412 R^*$  against the number of basis for a) donor impurity at the origin ( $d = 0 a^*$ ) and b) donor impurity at ( $d = 0.5 a^*$ ).

The basis wave functions are:

$$|n, m \rangle = \psi_{n,m}(\rho, \varphi) = \frac{1}{\sqrt{2\pi}} R_{n,m}(\rho) e^{im\varphi} \quad (5)$$

where,

$$R_{n,m}(\rho) = e^{-\frac{1}{2}\rho^2\alpha^2} \rho^{|m|} \alpha^{|m|} \sqrt{\frac{2\alpha^2 n!}{(n+|m|)!}} L_n^{|m|}(\rho^2\alpha^2) \quad (6)$$

and eigen energies

$$E_{n,m} = (2n + |m| + 1)\hbar\omega + m \frac{\omega c}{2} \quad (7)$$

where  $L_n^{|m|}(\rho^2\alpha^2)$  is the standard associated Laguerre polynomials [34]. And  $\alpha$  is an inverse length dimension constant which is given by:

$$\alpha = \sqrt{\frac{m\omega}{\hbar}} \quad (8)$$

Using these harmonic oscillator bases  $|n, m \rangle$ , the matrix elements of the full donor impurity Hamiltonian;  $\langle R_{n,m}(\rho) | \hat{H} | R_{i,m}(\rho) \rangle$ , can be diagonalized numerically to obtain the desired eigenenergies. In each calculation step the number of basis  $|n, m \rangle$  will be varied until a satisfied converging eigen energies are achieved. The stability converging procedure is displayed in Fig. 1.

The donor impurity binding energy (BE) which is defined as the difference between the energy states of the Hamiltonian (Eq. 1) without the presence of the impurity ( $E_0$ ) and with its presence ( $E$ ).

$$BE = E - E_0 \quad (9)$$

The effects of the pressure (P) and the temperature (T) on the energy of the ground state can be investigated using effective mass approximation method (EMA). The pressure and temperature dependence of the material electron effective mass,  $m^*(P, T)$  and dielectric constant  $\epsilon_r(P, T)$  are inserted in the impurity Hamiltonian as shown below

$$\hat{H}(\rho) = \frac{1}{2m^*(P, T)} \left[ \vec{p}(\rho) + \frac{e}{c} \vec{A}(\rho) \right]^2 + \frac{1}{2} m^*(P, T) \omega^2 \rho^2 - \frac{e^2}{\epsilon_r(P, T) \sqrt{\rho^2 + d^2}} \quad (10)$$

For quantum heterostructure made of GaAs the dielectric constant  $\epsilon_r(P, T)$  and the electron effective mass  $m^*(P, T)$  are presented by [10]

$$\epsilon_r(P, T) = \begin{cases} 12.74 \exp(-1.73 \times 10^{-3}P) \exp[9.4 \times 10^{-5}(T - 75.6)] & \text{for } T < 200 \text{ K} \\ 13.18 \exp(-1.73 \times 10^{-3}P) \exp[20.4 \times 10^{-5}(T - 300)] & \text{for } T \geq 200 \text{ K} \end{cases} \quad (11)$$

$$m^*(P, T) = \left[ 1 + 7.51 \left( \frac{2}{E_g^*(P, T)} + \frac{1}{E_g^*(P, T) + 0.341} \right) \right]^{-1} m_0 \quad (12)$$

$$E_g^*(P, T) = \left[ 1.519 - 5.405 \times 10^{-4} \frac{T^2}{T + 204} \right] + bP + cP^2 \quad (13)$$

Where  $m_0$  is the free electron mass,  $E_g^*(P, T)$  is the pressure and temperature dependent energy band gap for GaAs quantum heterostructure at  $\Gamma$  point,  $b = 1.26 \times 10^{-1} \text{ eV GPa}^{-1}$  and  $c = -3.77 \times 10^{-3} \text{ eV GPa}^{-2}$ .

The effective Rydberg in term of pressure and temperature is used as the energy unit.

$$R_y^*(P, T) = \frac{e^2}{2\epsilon(P, T) a_B^*(P, T)} \quad (14)$$

Where  $a_B^*(P, T)$  is the effective Bohr radius which given as:

$$a_B^*(P, T) = \frac{\epsilon(P, T) \hbar^2}{m^*(P, T) e^2} \quad (15)$$

Finally, the effective Rydberg can be written as:

$$R_y^*(P, T) = \frac{e^4 m^*(P, T)}{2(\epsilon(P, T))^2 \hbar^2} \quad (16)$$

Table (1) shows the variation of the material physical parameters, like effective mass and dielectric constant, in terms of the pressure and temperature.

## RESULTS AND DISCUSSIONS

For heterostructure system made from GaAs the material parameters are: dielectric constant  $\epsilon = 12.4$ , effective Rydber  $R^* = 5.926 \text{ meV}$  and

Table 1. The dependence of the physical parameters on the pressure and temperature.

	$m^*(P, T)$	$\epsilon_r(P, T)$
Pressure (P) $\uparrow \downarrow$	$\uparrow \downarrow$	$\downarrow \uparrow$
Temperature (T) $\uparrow \downarrow$	$\downarrow \uparrow$	$\uparrow \downarrow$

Table 2. The ground state ( $m=0$ ) energy (in  $R^*$ ) computed by the exact diagonalization method against  $\frac{1}{N}$  expansion method for various range of magnetic field strength ( $1\gamma = 6.75$  B (Tesla)).

$\gamma$	$B(\text{Tesla})$	$\omega_0 = 5.412 R^*$ Ground State Energy		$\omega_0 = 3.044 R^*$ Ground State Energy	
		ExactMethod	$\frac{1}{N}$ Method	ExactMethod	$\frac{1}{N}$ Method
1	6.75	-2.11017	-2.15	-3.12522	-3.29
2	13.5	-2.05033	-2	-2.94692	-3.11
3	20.25	-1.74839	-1.76	-2.67781	-2.8
3.5	23.625	-1.60974	-1.61	-2.50864	-2.61
4	27.	-1.4569	-1.44	-2.32688	-2.39
4.5	30.375	-1.27918	-1.26	-2.11917	-2.26
5	33.75	-1.0966	-1.06	-1.90787	-1.92

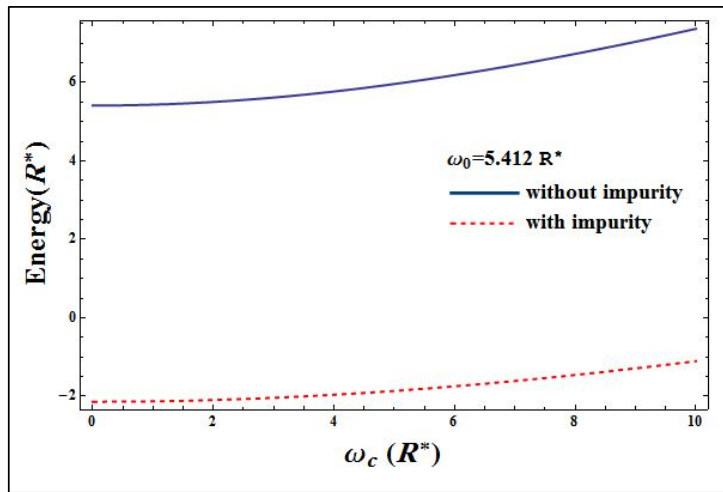


Fig. 2. The ground state energy of the quantum heterostructure for absence and presence of the impurity against the magnetic field strength  $\omega_c$  the dashed line with impurity and solid line for no impurity cases for  $\omega_0 = 5.412 R^*$ .

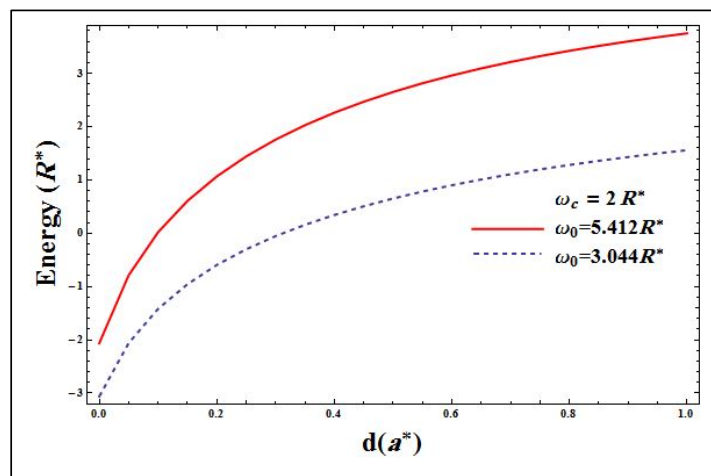


Fig. 3. The ground-state for fixed value of  $\omega_c = 2 R^*$  against the distance for two  $\omega_0$ , ( $\omega_0 = 3.044 R^*$  dashed line and  $\omega_0 = 5.412 R^*$  the solid line).

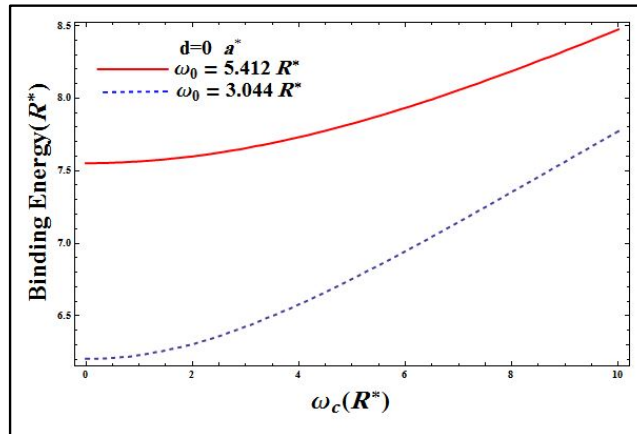


Fig 4.a

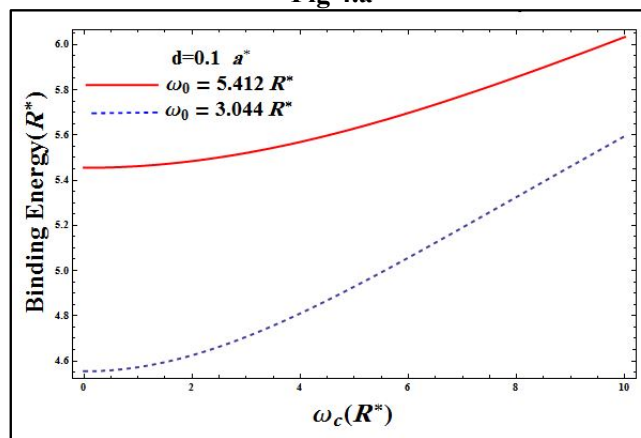


Fig 4.b

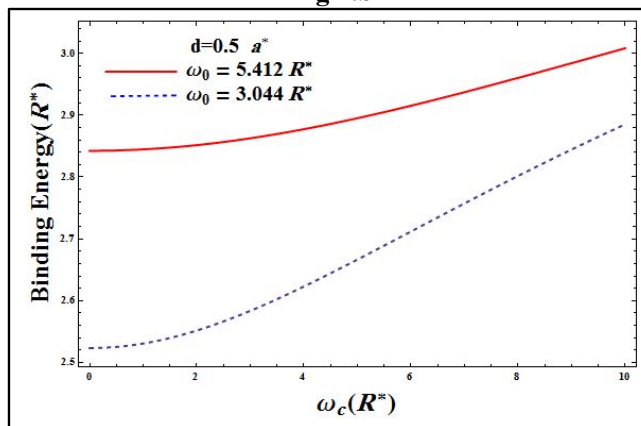


Fig 4.c

Fig. 4. The ground-state binding energy against  $\omega_c$ , where ( $\omega_0 = 3.044 R^*$  for dashed line, and  $\omega_0 = 5.412 R^*$  for solid line) (a)  $d = 0 a^*$ , (b)  $d = 0.1 a^*$ , and (c)  $d = 0.5 a^*$ .

the effective mass of an electron  $m^* = 0.067 m_e$  at ambient zero temperature and pressure. The impurity is located along z axis at the distance  $d$ , with the presence of a uniform external magnetic

field (B) along the z direction. In the first step we have calculated the ground state eigenenergy (where  $m=0$ ) for the donor impurity of GaAs/AlGaAs heterostructure as a function of the

Table 3. The donor impurity ground state energy ( $E(R^*)$ ), and donor impurity binding energy ( $BE(R^*)$ ) against the magnetic field strength  $\omega_c$  and various impurity position ( $d$ ) for  $\omega_0 = 3.044 R^*$ .

$\omega_c(R^*)$	$d=0 a^*$		$d=0.1 a^*$		$d=0.5 a^*$	
	$E(R^*)$	$BE(R^*)$	$E(R^*)$	$BE(R^*)$	$E(R^*)$	$BE(R^*)$
0.	-3.16072	6.20472	-1.50997	4.55397	0.520567	2.52343
0.5	-3.15595	6.21019	-1.50433	4.55858	0.528959	2.52529
1.	-3.14501	6.2298	-1.48746	4.57225	0.554005	2.53079
1.5	-3.12832	6.26336	-1.45957	4.5946	0.595315	2.53972
2.	-3.09887	6.30292	-1.42094	4.62499	0.652278	2.55177
2.5	-3.06943	6.36009	-1.372	4.66265	0.724104	2.56655
3.	-3.03356	6.42708	-1.31319	4.7067	0.809878	2.58364
3.5	-2.98742	6.4986	-1.24505	4.75624	0.90861	2.60258
4.	-2.93728	6.57952	-1.16812	4.81036	1.04276	2.62717
4.5	-2.87821	6.6635	-1.08295	4.86824	1.14089	2.6444
5.	-2.81585	6.75487	-0.990149	4.92918	1.27246	2.66656

Table 4. The donor impurity energy ( $E(R^*)$ ), and donor impurity binding energy ( $BE(R^*)$ ) against the magnetic field strength  $\omega_c$  and various impurity position ( $d$ ) for  $\omega_0 = 5.412 R^*$ .

$\omega_c(R^*)$	$d=0 a^*$		$d=0.1 a^*$		$d=0.5 a^*$	
	$E(R^*)$	$BE(R^*)$	$E(R^*)$	$BE(R^*)$	$E(R^*)$	$BE(R^*)$
0.	-2.14013	7.55213	-0.0426768	5.45468	2.56954	2.84246
0.5	-2.1377	7.55548	-0.0387892	5.45656	2.57473	2.84304
1.	-2.12914	7.56419	-0.0271437	5.46219	2.59026	2.84479
1.5	-2.11504	7.57876	-0.00779313	5.47151	2.61605	2.84767
2.	-2.09461	7.59822	0.0191767	5.48444	2.65196	2.85165
2.5	-2.07032	7.6248	0.0536489	5.50083	2.6978	2.85668
3.	-2.03883	7.65486	0.0954769	5.52055	2.75333	2.8627
3.5	-2.00289	7.69079	0.14449	5.54341	2.81827	2.86964
4.	-1.96213	7.73186	0.200496	5.56923	2.89231	2.87742
4.5	-1.91457	7.77565	0.263283	5.5978	2.97512	2.88596
5.	-1.86286	7.82438	0.332628	5.62889	3.06634	2.89518

magnetic field strength  $\omega_c$  with impurity located at the origin ( $d=0$ ) for two specific values of the confinement frequency strength  $\omega_0 = 5.412 R^*$ , and  $\omega_0 = 3.044 R^*$ . The accuracy of our obtained results are tested against the corresponding ones produced by  $\frac{1}{N}$  expansion method [35]. Table 2 shows the comparison between the ground state ( $m=0$ ) computed energy for the present exact diagonalization method and the available corresponding energy produced by  $\frac{1}{N}$  expansion method. The comparison shows a good agreement between both methods. To test the convergence issue of our exact diagonalization technique, we have plotted in Fig. 1a, 1b, the computed ground state energies ( $E$ ) of the donor impurity Hamiltonian against the number of basis ( $n$ ) from 1 to 38 for frequency  $\omega_0 = 5.412 R^*$ , impurity

distance  $d=0 a^*$  and  $0.5 a^*$ , and at magnetic field strength  $\omega_c = 2 R^*$ . The figures clearly show the numerical stability in our computed scheme. The ground state approaches a limiting value as the number of basis increases.

Fig. 2 displays the energy of the donor impurity energy as a function of the magnetic field strength  $\omega_c$ , for confinement frequency  $\omega_0 = 5.412 R^*$ . The solid plot of the system indicates the absence of the impurity, and the dashed one indicates the presence of the impurity. It is clear from Fig. 2 that the effect of the impurity is to decrease the energy of the system. The presence of donor impurity lowers the energy of the heterostructure energy due to its negative coulomb attraction.

The energy of the heterostructure shows a significant dependence on the impurity position. Increasing the impurity distance ( $d$ ), changing the system from 2D to 3D (bulk), as displayed clearly in

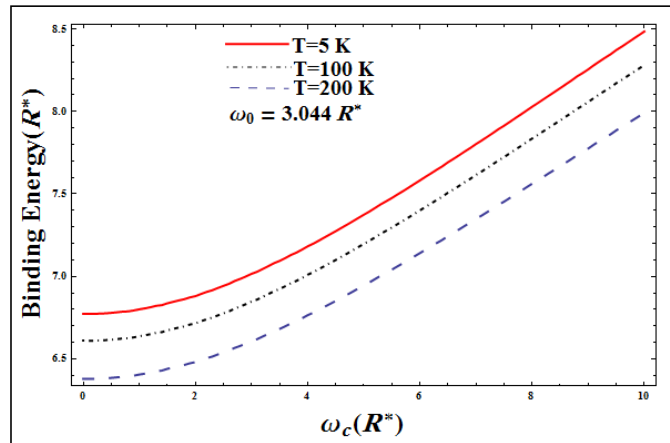


Fig. 5.a

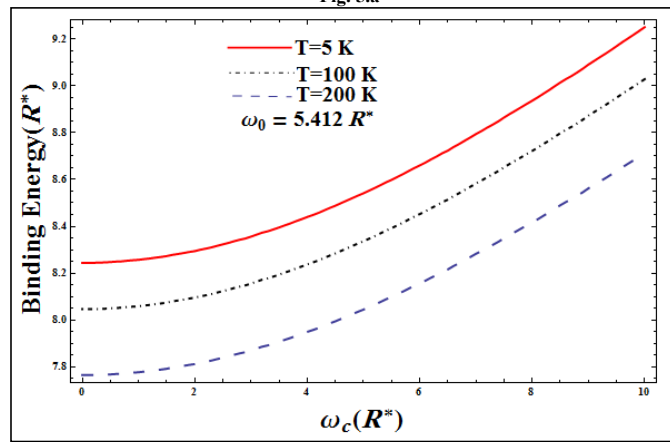


Fig. 5.b

Fig. 5. The binding energy for  $d=0 a^*$  at constant pressure ( $P=10\text{ kbar}$ ) as a function of  $\omega_c$  for three temperatures (5K, 100K, and 200K) for (a)  $\omega_0 = 3.044 R^*$  and b)  $\omega_0 = 5.412 R^*$ .

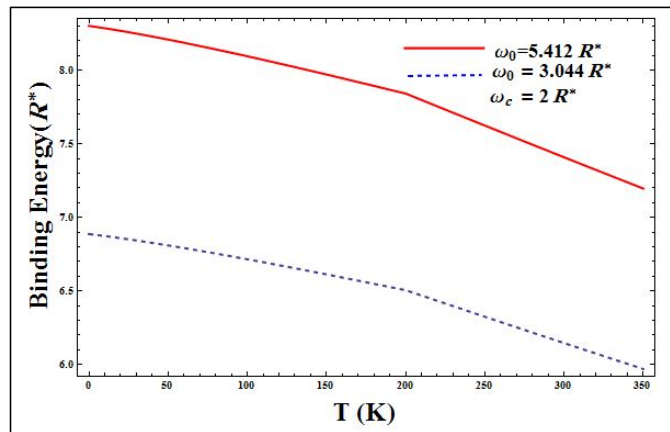


Fig. 6. The binding energy change for  $d=0 a^*$  at constant pressure ( $P=10\text{ kbar}$ ) and  $\omega_c = 2 R^*$  with respect to the temperature for ( $\omega_0 = 5.412 R^*$  solid line and for  $\omega_0 = 3.044 R^*$  for the dashed line).

Fig. 3. For fixed values of impurity position ( $d$ ), the energy of the donor Hamiltonian enhances as the confinement strength ( $\omega_0$ ) increases from 3.044

$R^*$  to 5.412 $R^*$ . This energy behavior agrees with our expectation.

Furthermore, we have investigated the impurity



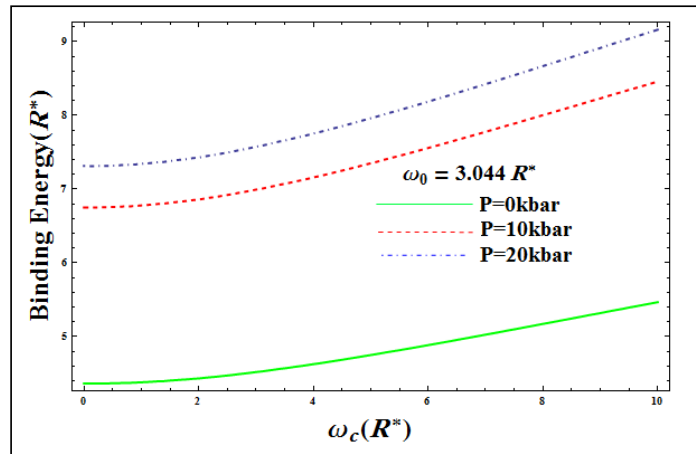


Fig.7.a

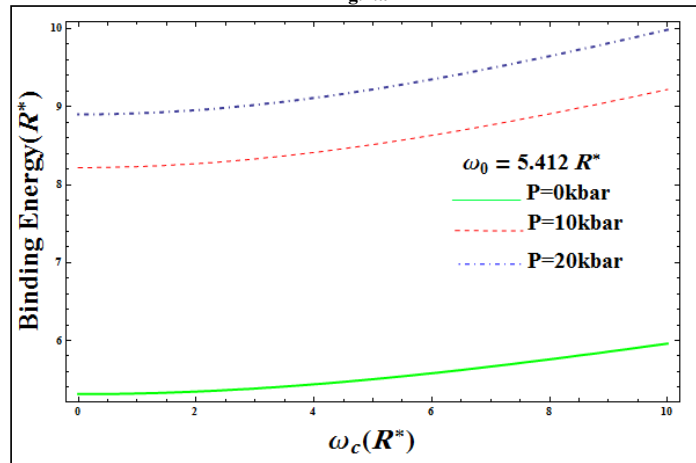


Fig.7.b

Fig. 7. The variation of ground-state binding energy for  $d=0a^*$  against the  $\omega_c$  at fixed temperature (20K) and for three different values of pressure (0, 10, and 20 kbar) a)  $\omega_0 = 3.044 R^*$  b)  $\omega_0 = 5.412 R^*$ .

ground -state eigenenergy (E) and the binding energy (BE) against the magnetic field strength  $\omega_c$ , for specific values of  $\omega_0$  and versus values of (d). Fig. 4a ,4b,4c,4d show the dependences of the ground state binding energy (BE) on the magnetic field strength  $\omega_c$  for different values of impurity distances : (a)  $d=0a^*$ , (b)  $d=0.1a^*$ , and (c)  $d=0.5a^*$  and two confinement frequencies ( $\omega_0 = 3.044 R^*$  and  $\omega_0 = 5.412 R^*$ ). The binding energy (BE), against the magnetic field strength, is greatly reduced as the distances (d) increases as shown by Figs. 2, 3 and 4. In addition, the figures demonstrate that the binding energy increases as magnetic field  $\omega_c$  and the parabolic confinement strengths  $\omega_0$  increase.

In Table 3, we have listed the donor impurity energy and binding energy as a function of

magnetic field strength  $\omega_c$  for  $\omega_0 = 3.044 R^*$  and for various values of d. For  $\omega_0 = 3.044 R^*$  and  $d=0 a^*$ , the binding energy increases as the magnetic field strength increases. This behavior persists for all d-values. However, the binding energy decreases as the impurity (d) increases. We can see a significant decrease in the binding energy as d increases from  $d=0.1 a^*$  to  $d=0.5 a^*$ . For example, at  $\omega_0 = 3.044 R^*$  and  $\omega_c = 2 R^*$  the binding energy reduces significantly from  $4.62499 R^*$  to  $2.55177 R^*$ . This result is due to the great reduction in the coulomb impurity energy (Eq. 4), as we mentioned earlier. The same qualitative behavior can also be observed in Table 4 with different quantitative behavior for  $\omega_0 = 5.412 R^*$ .

To see the effects of pressure and temperature parameters on the binding energy of the donor

impurity, we have inserted the pressure and temperature dependent material parameters of GaAs, ( $m^*(P,T)$  and  $\epsilon_r(P,T)$ ), in the present calculations. In Fig. 5 to Fig. 16, we have shown explicitly the behavior of the donor binding energy (BE) as a function of the magnetic field strength  $\omega_0$ , taking in consideration the impurity position ( $d$ ), temperature ( $T$ ), pressure ( $P$ ) and confinement frequency  $\omega_0$ . Fig. 5a, 5b show the donor binding energies against the magnetic field strength for three different temperatures (5K, 100K, and 200K) and fixed values of pressure, impurity position  $d=0 a^*$  and confinement frequency  $\omega_0 = 3.044 R^*$ . For fixed temperature, the figure clearly shows the enhancement of the binding energy as the magnetic field strength  $\omega_c$  increases. This enhancement in the donor binding energy can be attributed to the parabolic magnetic confinement term  $\frac{1}{4}\omega^2\rho^2$  in Eq. (3). For fixed values of magnetic field strength  $\omega_c$ , the binding energy decreases when the temperature increases, as clearly shown in Fig. 5a. Similar behavior of the donor binding energy is displayed in Fig. 5b for different,  $\omega_0 = 5.412 R^*$ .

In Fig. 6 we have shown the dependence of the donor binding energy on the temperature for fixed values of pressure ( $P=10$  Kbar),  $\omega_c = 2 R^*$ ,  $d = 0 a^*$  and various confinements  $\omega_0 = 3.044 R^*$  and  $\omega_0 = 5.412 R^*$ . The binding energy again shows a clear decreasing behavior as the temperature

of the system increases. The dependence of the material parameters like the effective mass  $m^*(P,T)$  and dielectric constant  $\epsilon_r(P,T)$  on the temperature and pressure explain in Table 1, where  $m^*$  decreases and  $\epsilon_r$  increases with increasing  $T$  which diminish donor impurity binding energy (BE).

In Fig. 7a, 7b, the behavior of the donor binding energy had been shown as a function of the magnetic field strength  $\omega_0$  for different values of parameters:  $\omega_0 = 5.412 R^*$  and  $\omega_0 = 3.044 R^*$ , pressure  $P=0, 10,$  and  $20$  kbar, impurity position  $d=0 a^*$ , and temperature  $T=20$  K. The donor binding energy shows a significant increase as the magnetic field  $\omega_c$  increases; as we increase the magnetic field strength  $\omega_c$ , the electron-atom separation distance decrease which in turn increases the electron confinement. The binding energy again shows a great enhancement as the pressure increases, while keeping the magnetic field strength unchanged.

In Fig. 8, we take the temperature  $T=20$ K,  $\omega_c = 2R^*$  and  $d = 0 a^*$  parameters, while changing the pressure. We observe a great enhancement in the donor binding energy as the pressure increases for confinement strength:  $\omega_0 = 3.044 R^*$  and  $\omega_0 = 5.412 R^*$ . This behavior is expected; since as we increase the pressure, the effective mass  $m^*$  increases while the dielectric constant  $\epsilon_r$  decreases. These changes in the material parameters lead to a reduction in the kinetic energy of the electron while the attractive

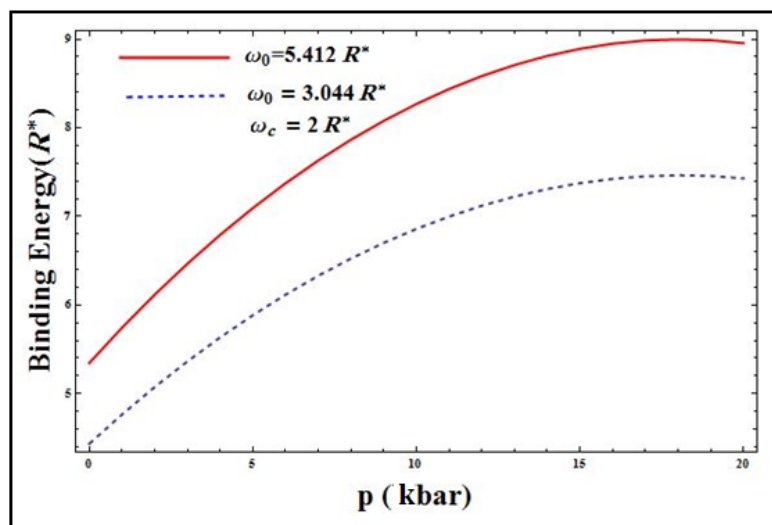


Fig. 8. The variation of ground-state binding energy for  $d = 0 a^*$  against the pressure at fixed temperature (20K) and  $\omega_c = 2 R^*$  for ( $\omega_0 = 3.044 R^*$  and  $\omega_0 = 5.412 R^*$ ).

coulomb energy of the electron enhances.

In Fig.9a and 9b, we have shown the effect of changing the temperature, at fixed value of the impurity position ( $d= 0.1 a^*$ ), on the binding energy. Again, the binding energy shows great enhancement as we increase the magnetic field strength  $\omega_c$  for fixed values of the parameters: Temperature ( $T= 5, 100,$  and  $200K$ ), Pressure ( $P=10$  kbar) and confinement frequencies  $\omega_0 = 3.044 R^*$  and  $\omega_0 = 5.412 R^*$ . We display in Fig. 10 the donor binding energy against the temperature ( $T$ ), while the rest of the physical parameters of the system are kept fixed. The binding energy shows an important dependence on the temperature, and

the impurity binding energy  $E_B$  decreases with increasing the temperature.

In Fig. 11a and 11b, the pressure effect on the donor binding energy for  $d=0.1 a^*$  against the magnetic field strength  $\omega_c$  had been illustrated. Fig. 11a obviously shows that the binding energy increases as the magnetic field strength enhances while the pressure ( $0, 10,$  and  $20$  kbar),  $T, d,$  and  $\omega_0 = 3.044 R^*$  are fixed. Fig. 11b shows similar behavior of the (BE) but for different confinement  $\omega_0 = 5.412 R^*$ . Effective-mass approximation investigates the pressure effects on  $m^*$  and  $\epsilon_r$ , as shown in Table 1 which explain the reason of enhancing BE.

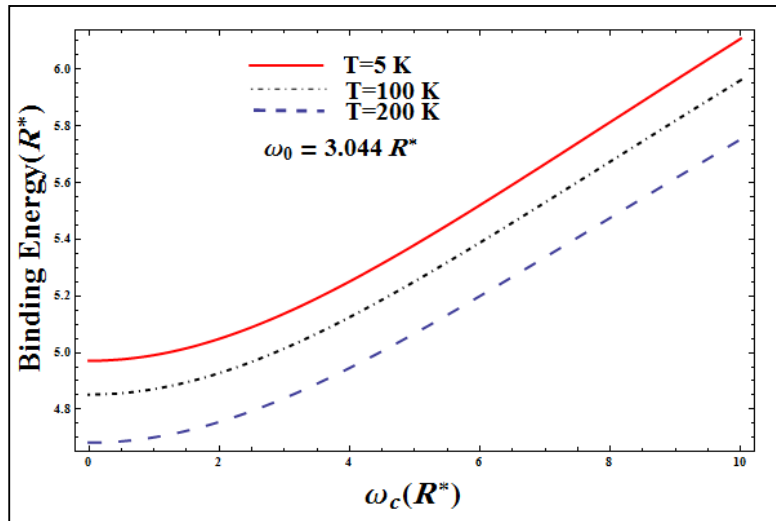


Fig. 9.a

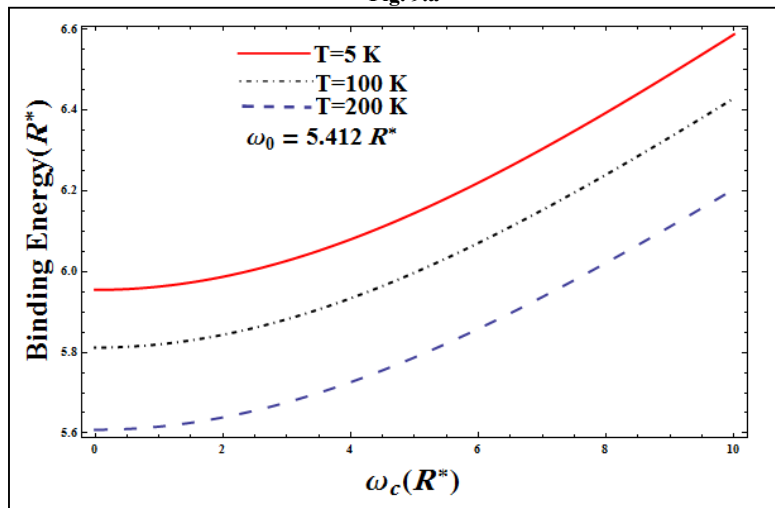


Fig. 9.b

Fig. 9. The ground-state binding energy for  $d=0.1 a^*$  at constant pressure ( $P=10$  kbar) as a function of  $\omega_c$  and for three temperatures (5K, 100K, and 200K):

a)  $\omega_0 = 3.044 R^*$  and b)  $\omega_0 = 5.412 R^*$ .

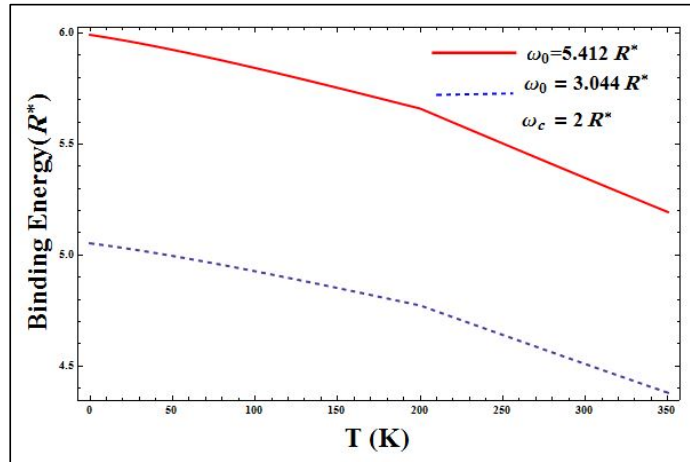


Fig. 10. The ground-state binding energy for  $d = 0.1 a^*$  at constant pressure ( $P = 10$  kba and  $\omega_c = 2 R^*$ ), and temperature for ( $\omega_0 = 3.044 R^*$  dashed line and  $\omega_0 = 5.412 R^*$  for the solid line).

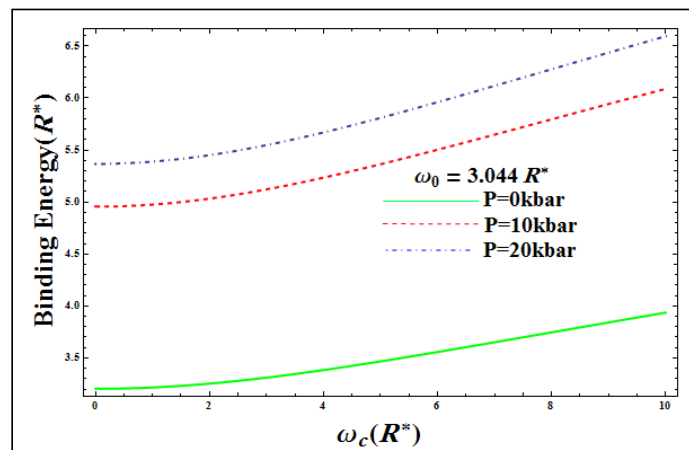


Fig. 11.a

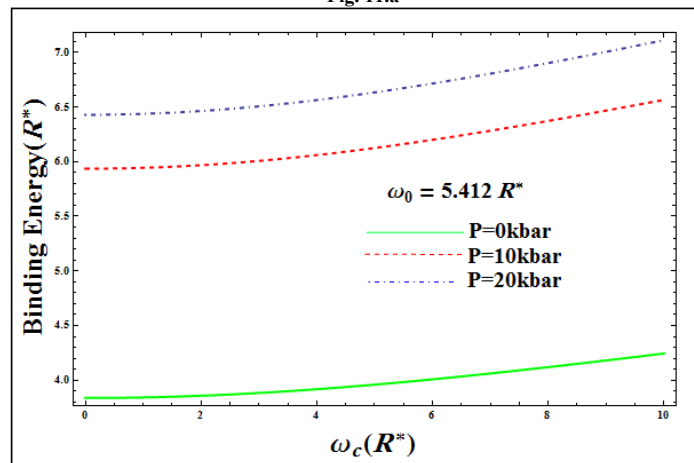


Fig. 11.b

Fig. 11. The variation of binding energy for  $d = 0.1 a^*$  against the  $\omega_c$  at fixed temperature (20K) for three pressure values (0, 10, and 20 kbar) a) for  $\omega_0 = 5.412 R^*$  b) and for  $\omega_0 = 3.044 R^*$ .

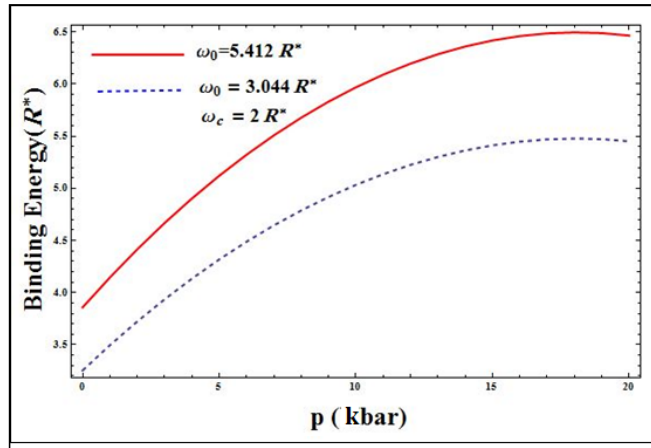


Fig. 12. The variation of ground-state binding energy for  $d=0.1 a^*$  as a function of the pressure at fixed temperature (20K) and  $\omega_c = 2 R^*$  for  $\omega_0 = 3.044 R^*$  and  $\omega_0 = 5.412 R^*$ .

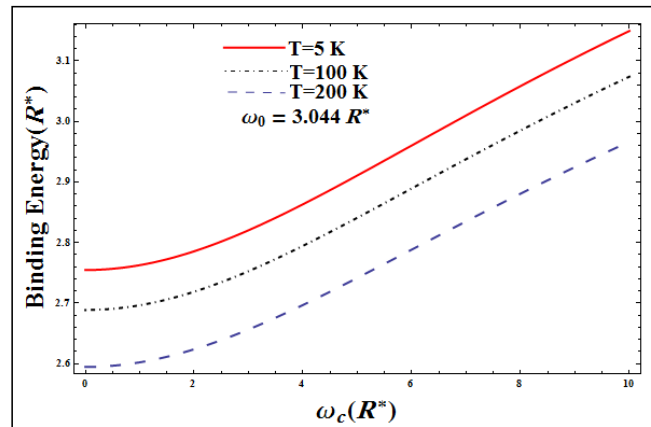


Fig. 13.a

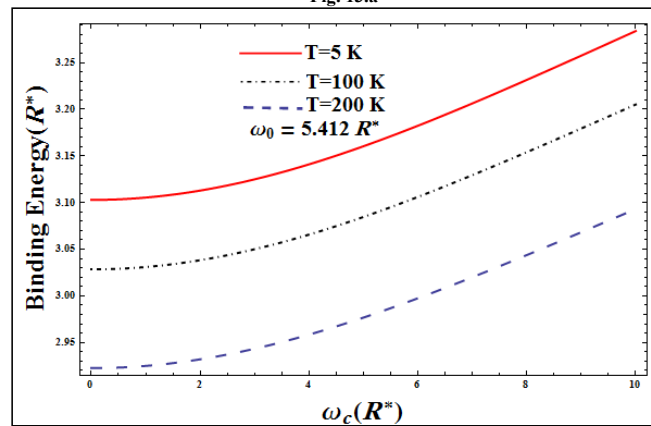


Fig.13.b

Fig. 13. The binding energy for  $d=0.5 a^*$  at constant pressure ( $P=10$  kbar) as a function of  $\omega_c$  for three temperatures (5K, 100K, and 200K). a)  $\omega_0 = 3.044 R^*$  and b)  $\omega_0 = 5.412 R^*$ .

In Fig. 12, the ground state binding energy as a function of the pressure for fixed values of  $T=20K$ ,  $d = 0.1 a^*$ ,  $\omega_c = 2R^*$  and at different confinements:  $\omega_0 = 3.044 R^*$  and  $\omega_0 = 5.412 R^*$

had been plotted. The binding energy, (BE) shows a great enhancement as the pressure increases for fixed values of confinement frequency because of increasing  $m^*$  and decreasing  $\epsilon_r$ . This effective

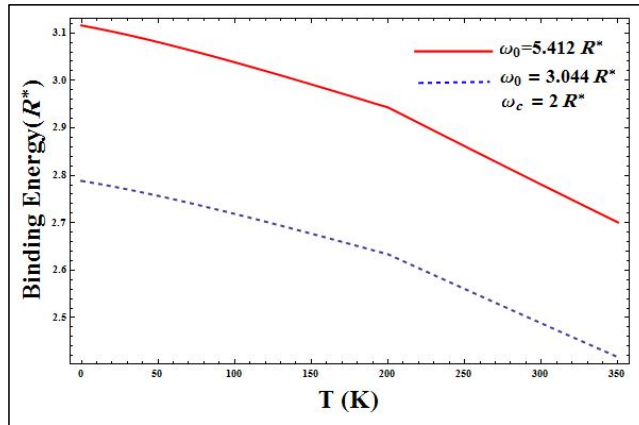


Fig. 14. The binding energy for  $d=0.5 a^*$  at constant pressure ( $P=10$  kbar) and  $\omega_c = 2 R^*$  against temperature for ( $\omega_0 = 3.044 R^*$  for the dashed line and for  $\omega_0 = 5.412 R^*$  solid line).

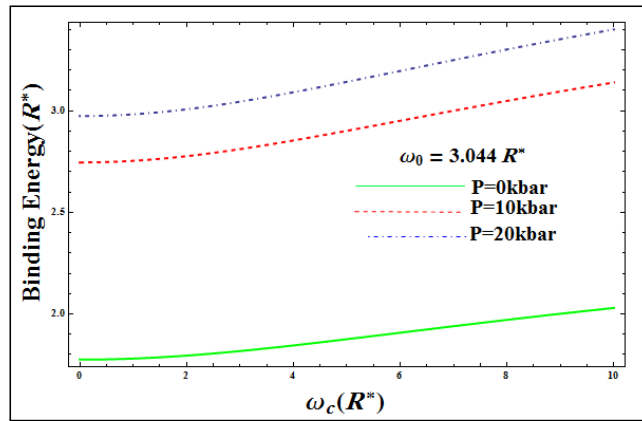


Fig. 15.a

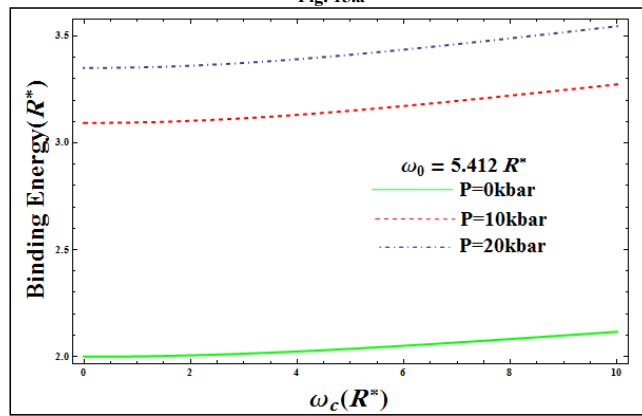


Fig. 15.b

Fig. 15. The binding energy for  $d=0.5 a^*$  against the  $\omega_c$  at fixed temperature (20 K) for three pressure values (0, 10, and 20 kbar): a) for ( $\omega_0 = 3.044 R^*$ ) b) and  $\omega_0 = 5.412 R^*$ .

mass and dielectric pressure dependence lead to lower the electron kinetic energy while the coulomb energy increases.

Fig. 13a and 13b, the binding energy as a

function of magnetic field strength for  $d=0.5 a^*$  and various confinement, had been shown. We have plotted in Fig. 14 the dependence of the donor binding energy against the temperature

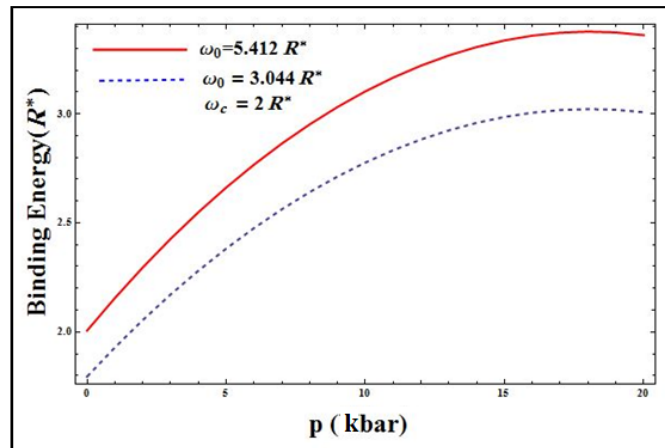


Fig. 16. The variation of ground-state binding energy for  $d = 0.5 a^*$  against the pressure at fixed temperature (20K) and  $\omega_c = 2$  for  $\omega_0 = 3.044 R^*$  and  $\omega_0 = 5.412 R^*$ .

for  $d=0.5 a^*$  and various confinement frequencies  $\omega_0 = 3.044 R^*$  and  $\omega_0 = 5.412 R^*$  and the rest parameter are fixed. The behavior is in qualitative agreement with the results explained in Fig. 6.

In Fig. 15a and 15b, we show similar qualitative behaviors as given in Figs. 3.10 a and b ( $d=0 a^*$ ). Fig. 15a and 15b show the effect of pressure and impurity position ( $d=0.5 a^*$ ) on the (BE) as a function of magnetic field strength. The comparison between two  $d$ -values ( $d=0$  and  $0.5 a^*$ ) show that, as we increase,  $d$ , the binding energy increases due to the great reduction in the coulomb attraction energy (Eq. 4). In Fig.16, we display the results of the donor binding energy for  $d=0.5 a^*$ . The behavior shown agrees with the (BE) behavior given in Fig.8 (for  $d=0 a^*$  with same reason).

## CONCLUSION

In conclusion, the exact diagonalization method had been used to solve the donor impurity Hamiltonian in a heterostructure subjected to an applied magnetic field. The ground-state energy of GaAs/AlGaAs heterostructure had been computed. Furthermore, the impurity effect on the ground-state energy had been shown. In addition, the influence of the hydrostatic pressure, temperature and magnetic field on the binding energy of the donor impurity can be summarized as follows: the donor impurity binding energy is a decreasing function of temperature for fixed values of pressure and magnetic field. For example the donor impurity binding energy decrease from  $BE=8.3 R^*$  to  $BE= 7.8 R^*$  as we

increase the temperature from  $T=5K$  to  $T= 200 K$ , respectively calculated at  $\omega_c=2.0 R^*$ ,  $\omega_0 = 5.412 R^*$  and pressure  $P=10$  Kbar. Also the donor impurity binding energy is increasing function of pressure for fixed values of temperature and magnetic field. For strong magnetic field strength, the donor binding energies enhances significantly for any hydrostatic pressure and temperature values as we expected.

## CONFLICT OF INTEREST

The authors declare that they have no competing interests.

## REFERENCES

- [1] Bastard G., (1981), Hydrogenic impurity states in a quantum well: A simple model. *Phys. Rev. B.* 24: 4714-4718.
- [2] Poonam V., Sanjiv K. M., (2019), Applications of silver nanoparticles in diverse sectors. *Int. J. Nano. Dimens.*10: 18-36.
- [3] Porras-Montenegro N., Perez-Merchancano S., Iatje A., (1993), Binding energies and density of impurity states in spherical GaAs-(Ga, Al)As quantum dots. *J. Appl. Phys.* 74: 7624-7628.
- [4] Ciftja O., (2013), Understanding electronic systems in semiconductor quantum dots, *Phys. Scrip.* 88: 058302-058306.
- [5] Liang S., Xie W. F., (2011), The hydrostatic pressure and temperature effects on a hydrogenic impurity in a spherical quantum dot. *Eur. Phys. J. B.* 81: 79-84.
- [6] Holtz O., Qing Xiang Zh., (2004), Impurities confined in quantum structures, 1st ed, (*Springer*), 5-10.
- [7] Dingle R., Stormer H. L., Gossard A. C., Wiegmann W., (1978), Electron mobilities in modulation-doped semiconductor heterojunction superlattices. *Appl. Phys. Lett.* 33: 665-671.
- [8] Zhu J.-L., (1989), Exact solutions for hydrogenic donor states in a spherically rectangular quantum well. *Phys. Rev. B.* 39: 8780-8786.

- [9] Yuan J.-H., Liu Ch., (2008), Binding energy of an off-center hydrogenic donor in a spherical quantum dot with strong parabolic confinement. *Phys. E*. 41: 41-44.
- [10] Rezaei G., Shojaeian Kish S., (2012), Effects of external electric and magnetic fields, hydrostatic pressure and temperature on the binding energy of a hydrogenic impurity confined in a two-dimensional quantum dot. *Phys. E: Low-dimens. Sys. Nanostruc.* 45: 56-60.
- [11] Zhu J., Cheng Y., Xiong J., (1990), Exact solutions for two-dimensional hydrogenic donor states in a magnetic field. *Phys. Lett. A*. 145: 358-362.
- [12] Mmadi A., Ahmani K. R., Zorkani I., Jorio A., (2013), Diamagnetic susceptibility of a magneto-donor in Inhomogeneous Quantum Dots. *Superlat. Microstruct.* 57: 27-36.
- [13] Miller D. A. B., Chemla D. S., Schmitt-Rink S., (1987), Relation between electroabsorption in bulk semiconductors and in quantum wells: The quantum-confined Franz-Keldysh effect. *Phys. Rev. B*. 33: 6976-6980.
- [14] Chen H., Li X., Zhou Sh., (1991), Stark shift of hydrogenic impurity states in a quantum well. *Phys. Rev. B*. 4: 6220-6226.
- [15] MacDonald A. H., Ritchie D. S., (1986), Hydrogenic energy levels in two dimensions at arbitrary magnetic fields. *Phys. Rev. B*. 33: 8336-8341.
- [16] Chuu D. S., Hsiao C. M., Mei W. N., (1992), Hydrogenic impurity states in quantum dots and quantum wires. *Phys. Rev. B*. 46: 3898-3904.
- [17] Zhu K. D., Gu S. W., (1993), Shallow donors in a harmonic quantum dot in high magnetic fields. *Phys. Lett. A*. 172: 296-298.
- [18] Khordad R., Fathizadeh N., (2012), Simultaneous effects of temperature and pressure on diamagnetic susceptibility of a shallow donor in a quantum antidote. *Physica. B*. 407: 1301-1305.
- [19] John P. A., (2008), Simultaneous effects of pressure and magnetic field on donors in a parabolic quantum dot. *Solid State Commun.* 147: 296-300.
- [20] Perez-Merchancano S. T., Paredes-Gutierrez H., Silva-Valencia J., (2006), Hydrostatic-pressure effects on the donor binding energy in GaAs-(Ga, Al)As quantum dots. *J. Phys: Condens. Matter*. 19: 026225-026230.
- [21] Kassim H. A., (2007), Study of shallow donor level binding energies confined in a GaAs-Ga<sub>1-x</sub>Al<sub>x</sub>As spherical quantum dot. *J. Phys: Condens. Matter*. 19: 036204-036209.
- [22] Bzour F., Shaer A., Elsaid Mohammad K., (2017), The effects of pressure and temperature on the exchange energy of a parabolic quantum dot under a magnetic field. *J. Taibah Univ. Sci.* 11: 1122-1134.
- [23] Schwarz M. P., Grundler D., Wilde D. M., Heyn M. Ch., Heitmann D. J., (2002), Magnetization of semiconductor quantum dots. *J. Appl. Phys.* 91: 6875-6877.
- [24] Hijaz E., Elsaid M. K., Elhassan M., (2017), Magnetization of coupled double quantum dot in magnetic fields. *J. Comput. Theor. Nanosc.* 14: 1700-1705.
- [25] Bzour F., Elsaid M. K., Ilaiwi K. F., (2018), The effects of pressure and temperature on the energy levels of a parabolic two-electron quantum dot in a magnetic field. *J. King Saud. Univ.* 30: 83-90.
- [26] Bzour F., Elsaid M. K., Shaer A., (2017), The effects of pressure and temperature on the magnetic susceptibility of semiconductor quantum dot in a magnetic field. *App. Phys. Res.* 9: 77-82.
- [27] Elsaid M., Hijaz E., (2017), Magnetic susceptibility of coupled double GaAs quantum dot in magnetic fields. *Acta Phys. Pol. A*. 131: 1491-1496.
- [28] Elsaid M., Hjaz E., (2017), Energy states and exchange energy of coupled double quantum dot in a magnetic field. *Int. J. Nano Dimens.* 8: 1-8.
- [29] Shaer A., Elsaid M., Elhasan M., (2016), The magnetic properties of a quantum dot in a magnetic field. *Turk. J. Phys.* 40: 209-218.
- [30] Shaer A., Elsaid M., Elhasan M., (2016), Variational calculations of the heat capacity of a semiconductor quantum dot in magnetic fields. *Chin. J. Phys.* 54: 391-397.
- [31] Shaer A., Elsaid M., Elhasan M., (2016), Variational calculations of the exchange energy of a two-electron quantum dot in a magnetic field. *Jord. J. Phys.* 9: 87-93.
- [32] Shaer A., Elsaid M., Elhasan M., (2016), Magnetization of GaAs parabolic quantum dot by variation method. *J. Phys. Sci. App.* 6: 39-46.
- [33] Bruno-Alfonso A., Candido L., Hai G-Q., (2010), Two-dimensional electron states bound to an off-plane donor in a magnetic field. *J. Phys: Condens. Matter*. 22: 125801-125806.
- [34] Khajeh Salehani H., Shakouri Kh., Esmaeilzadeh M., Majlesara M. H., (2012), Effects of on-center impurity on energy levels of low-lying states in concentric double quantum rings. *Int. J. Nano Dimens.* 3: 43-51.
- [35] El-Said M., (1994), Effects of applied magnetic field on the energy Levels of shallow donors in a parabolic quantum dot. *Phys. B: Condens. Matter*. 202: 202-206.